 CMC, vol.26, no.3, pp.227-253, 2011

H-Adaptive Local Radial Basis Function Collocation Meshless Method

G. Kosec[1] **and B. Šarler**[1,2]

Abstract: This paper introduces an effective H-adaptive upgrade to solution of the transport phenomena by the novel Local Radial Basis Function Collocation Method (LRBFCM). The transport variable is represented on overlapping 5-noded influence-domains through collocation by using multiquadrics Radial Basis Functions (RBF). The involved first and second derivatives of the variable are calculated from the respective derivatives of the RBFs. The transport equation is solved through explicit time stepping. The H-adaptive upgrade includes refinement/derefinement of one to four nodes to/from the vicinity of the reference node. The number of the nodes added or removed depends on the topology of the reference node vicinity. The refinement/derefinement is triggered by an error indicator, which very simply depends on the ratio between the norm of the collocation coefficients and collocation matrix. The refinement/derefinement is proportional with the growth/decay of this indicator. Such adaptivity much increases the accuracy/performance ratio of the method. The performance of the method is numerically tested on two-dimensional Burger's equation. The results are compared with different numerical solutions, published in literature. Outstanding CPU efficiency and accuracy are clearly demonstrated from the results. The paper probably for the first time shows such a simple and effective H-adaptive meshless method, designed on five noded influence domain. The advantages of the represented meshless approach are its simplicity, accuracy, similar coding in 2D and 3D, straightforward applicability in non-uniform node arrangements, and native parallel implementation.

Keywords: Meshless method, collocation, radial basis functions, explicit time stepping, error indicator, Hardy's multiquadrics, H-adaptive node distribution, Burger's equation.

[1] University of Nova Gorica

[2] Centre of Excellence for Biosensors, Instrumentation and Process Control, E-mail: bozidar.sarler@ung.si

1 Introduction

Meshless methods for solving continuum mechanics [Liu and Gu, (2001); Atluri, (2004); Fasshauer, (2006)] and cellular automata based [Lorbiecka and Šarler, (2010)] physical models represent one of the most progressing research discipline, positioned between applied mathematics and computational engineering. A central point of any meshless (or sometimes also named meshfree or mesh reduction) method represents multivariate scattered data fitting and afterwards calculation of derivatives or integrals based on it. The numerical methods, designed on these principles can easily and in an ordered way handle different dimensions, irregular and moving boundaries, by avoiding any additional geometrical constructions (mesh) between the nodal nodes. There exists a large spectrum of meshless methods, depending on the type of multivariate data fitting and formulation design. The multivariate data fitting can be made by polynomials, radial basis functions, etc, and the formulation can originate from the strong, weak and weak-strong formulation. The weak forms are usually more stable on the expense of the background mesh for performing the integration of the shape and weight functions forms. Typical examples of the weak forms are Element free Galerkin method, Meshless Petrov-Galerkin method [Atluri and Shen, (2002); Atluri, (2004); Trobec, Sterk and Robic, (2009)], typical examples of the strong forms are SPH [Monaghan, (1988)], DAM [Prax, Sadat and Salagnac, (1996)] and Kansa method [Kansa, (1990a); Kansa, (1990b)], and a typical example of weak-strong forms is [Liu, Wu and Ding, (2004)].

The present work is focused on one of the simplest classes of meshless methods in development today, the Local Point Interpolation [Wang and Liu, (2002)] Radial Basis Function [Buhmann, (2000)] Collocation Method (RBFCM) [Šarler, (2007)]. This method is additionally generalized and upgraded in order to be able to apply it in the adaptive node distribution sense. The original, global version of the RBF collocation method, has been applied in different scientific and engineering problems from heat transport [Zerroukat, Power and Chen, (1998)] and convective diffusive problems [Šarler, Perko and Chen, (2004)] to the fluid flow problems [Šarler, Perko, Chen and Kuhn, (2001); Divo and Kassab, (2007)], phase change phenomena [Kovačevič, Poredoš and Šarler, (2003)], wave equations [Haq, ul-Islam and Arshed, (2008)] and solid mechanics problems [Mai-Duy, Khennane and Tran-Cong, (2007); Le, Mai-Duy, Tran-Cong and Baker, (2008); Sorić and Jarak, (2010)]. The method has been formulated by integrating the partial derivatives [Mai-Duy and Tran-Cong, (2003)] and applied to transient problems [Mai-Cao and Tran-Cong, (2005)], fluid flow [Mai-Duy, Mai-Cao and Tran-Cong, (2007)] and moving boundaries [Mai-Cao and Tran-Cong, (2008)]. Several improvements have been applied such as the advanced Neumann boundary conditions treatment [Libre, Emdadi, Kansa, Rahimian and Shekarchi, (2008)] or double consideration of

the boundary nodes [Šarler, (2005)]. The main drawback of this global method originates in the need for solving the global matrices in order to solve the problem. The condition number of the global matrix is highly sensitive to the shape of the basis functions and the node distribution, as well. The problem becomes important even with a relatively small number of the nodes ($\approx$1000). The mitigation of the related problem has been attempted by domain decomposition [Mai-Duy and Tran-Cong, (2002)], multi-grid approach and compactly supported RBFs [Chen, Ganesh, Golberg and Cheng, (2002)] which all represent a substantial complication of the original simple method. A substantial breakthrough in the development of the RBFCM was its local formulation for boundary value problems (LRBFCM) by Lee at al. [Lee, Liu and Fan, (2003)]. They demonstrated that the local formulation does not substantially degrade the accuracy with respect to the global one. On the other hand, it is much less sensitive to the choice of the RBF shape parameter and node distribution. The local RBFCM, where the collocation is made piecewise on the influence domains, has been previously developed for diffusion problems [Šarler and Vertnik, (2006)], convection-diffusion solid-liquid phase change problems [Vertnik and Šarler, (2006)] and subsequently successfully applied in industrial process of direct chill casting [Vertnik, Založnik and Šarler, (2006)]. The engineering k-epsilon turbulence modeling was implemented by [Vertnik and Šarler, (2009)]. The LRBFCM represents a local variant of the global RBFCM (or Kansa method) for thermo-fluid problems [Šarler, Perko, Chen and Kuhn, (2001); Šarler, (2005)]. LRBFCM is equivalent to Kansa method in case there is only one influence domain and it extends over the entire calculation domain.

Different adaptive strategies (modifications of space and time discretization) have been used in the past in connection with different numerical methods to enhance the numerical effectiveness of computation. In general, the refinement schemes can be classified into three major categories, which are h-refinement, p-refinement and r-refinement. The h-refinement scheme, tackled in the continuation of this paper, changes the number of the node and its neighboring nodes by insertion or removal of the nodes, based on error indicator. This strategy has been already introduced into global RBFCM [Libre, Emdadi, Kansa, Shekarchi and Rahimian, (2008); Bourantas, Skouras and Nikiforidis, (2009); Ling, (2011)]. In the context of the local methods, only local least squares approximation has been used, in connection with the Delaunay triangulation [Park, C. and K., (2003)] [Liu, Huynh and Gu, (2006)], [Liu, Kee and Lu, (2006); Kee, Liu and Lu, (2008)]. The adaptive calculations have been made by reproducing kernel particle method for cracks in [Rabczuk and Belytschko, (2005)] and large deformation problems in [Gan, Li and Long, (2009)]. Adaptive calculations by using RBF have been used in the context of mixed Eulerian-Lagrangean formulation by [Behrens and Iske, (2002)]. By the

best knowledge of the present authors, an adaptive method with a simple 5-noded LRBFCM has not yet been introduced.

In the p-refinement scheme, one increases the order of the approximation. This in the meshless methods means increase of the number of shape functions, modifications of the shape functions and/or increase of the influence domain size [Stevens, Power, Lees and Morvan, (2009)]. The r-refinement [Li, Petzold and Ren, (1998); Mencinger, (2003); Kovačevič and Šarler, (2005); Perko and Šarler, (2007)] keeps the total number of the nodes unchanged, but adjusts their position to obtain an optimal approximation [Shanazari and Rabie, (2009)]. The node distribution density is controlled by moving the nodes into the regions of intense changes in the fields. There are various ways to achieve the suitable moving. The most popular one is to solve additional equations to control the node distribution density. The drawback of such an approach represents the limitation of the number of computational nodes. Therefore, one part of the domain might be covered with fewer nodes than needed in order to satisfy the needs of the other regions.

The simplest possible h-adaptive approach in 2D is to subdivide the rectangular stencil (FDM) or cell (FVM) to four new nodes [Berger, (1983); Berger and Colella, (1989)]. It is easy, in general, to add nodes in meshless methods, since a corresponding polygon (mesh) structure need not be developed.

The organization of the rest of the paper is as follows. Governing transport equation is introduced. LRBFCM is explained. The node refinement and derefinement is discussed. Error estimator is introduced. A numerical example with Burger's equation is elaborated. The advantages and limitations of the method are analyzed, together with the discussion on future work.

2 Governing equations

Let us focus our discussion to solution of the general transport equation, defined on a fixed domain Ω with boundary Γ, standing for a reasonably broad spectra of mass, energy, momentum, and species transfer problems

$$\frac{\partial \Phi(\mathbf{p},t)}{\partial t} = \nabla \cdot (D(\mathbf{p},t)\nabla\Phi(\mathbf{p},t)) - \nabla \cdot (\rho \mathbf{v}(\mathbf{p},t)\Phi(\mathbf{p},t)) + S(\mathbf{p},t) \tag{1}$$

with $\rho, \Phi, t, \mathbf{p}, \mathbf{v}, D$, and S standing for density, transport variable, time, position vector, velocity, diffusion coefficient and source, respectively. The solution of the governing equation for the transport variable at the final time $t_0 + \Delta t$ is sought, where t_0 represents the initial time and Δt the positive time increment. The solution is constructed by the initial and boundary conditions that follow. The initial value of the transport variable $\Phi(\mathbf{p},t)$ at a node with position vector $\mathbf{p}$ and time t_0 is

defined through the known function Φ_0

$$\Phi(\mathbf{p},t) = \Phi_0(\mathbf{p},t); \quad \mathbf{p} \in \Omega + \Gamma \tag{2}$$

The boundary Γ is divided into not necessarily connected parts $\Gamma = \Gamma^D \cup \Gamma^N$ with Dirichlet and Neumann type boundary conditions, respectively. At the boundary node $\mathbf{p}$ with normal $\mathbf{n}_\Gamma$ and time $t_0 \leq t \leq t_0 + \Delta t$, these boundary conditions are defined through known functions Φ_Γ^D, Φ_Γ^N

$$\Phi = \Phi_\Gamma^D; \quad \mathbf{p} \in \Gamma^D \tag{3}$$

$$\frac{\partial}{\partial n_\Gamma}\Phi = \Phi_\Gamma^N; \quad \mathbf{p} \in \Gamma^N \tag{4}$$

3 LRBFCM

The local meshless method, used in this paper for solving the above transport equation, is based on strong formulation and explicit time stepping. Spatial disretization is performed through local collocation of the transport variable by RBF's, followed by application of partial differential operator on the collocation function. Such approach has been successfully tested in several thermo-fluid problems [Kosec and Šarler, (2008b); Kosec and Šarler, (2008a); Sanyasiraju and Chandhini, (2008); Kosec and Šarler, (2009); Vertnik and Šarler, (2009); Vertnik and Šarler (2011)] as well as other computations [Šarler, Kosec, Lorbiecka and Vertnik, (2009); Lorbiecka and Šarler, (2010)]. This most simple version of the approach can be altered by using moving least squares (MLS) instead of collocation, and instead of RBFs any kind of other basis functions. The MLS approach with monomial basis is in literature referred as the Diffuse Approximate Method (DAM) [Prax, Sadat and Salagnac, (1996); Perko and Šarler, (2007); Trobec, Kosec, Šterk and Šarler, (2012)] and represents an alternative for LRBFCM. Due to the completely local behavior, LRBFCM exhibits several convenient advantages such as ease of implementation, straightforward parallelization, simple consideration of complex physical models and CPU effectiveness.

The main idea behind the local meshless numerical approach is the use of a local influence domain for approximation of an arbitrary field in order to evaluate the differential operators needed to solve the partial differential equations. The principle is represented in Figure 1.

Each node uses its own influence domain for spatial differential operations; the domain is therefore discretized with overlapping influence domains. The approximation function is introduced as

$$\theta(\mathbf{p}) = \sum_{n=1}^{N} \alpha_n \Psi_n(\mathbf{p}), \tag{5}$$

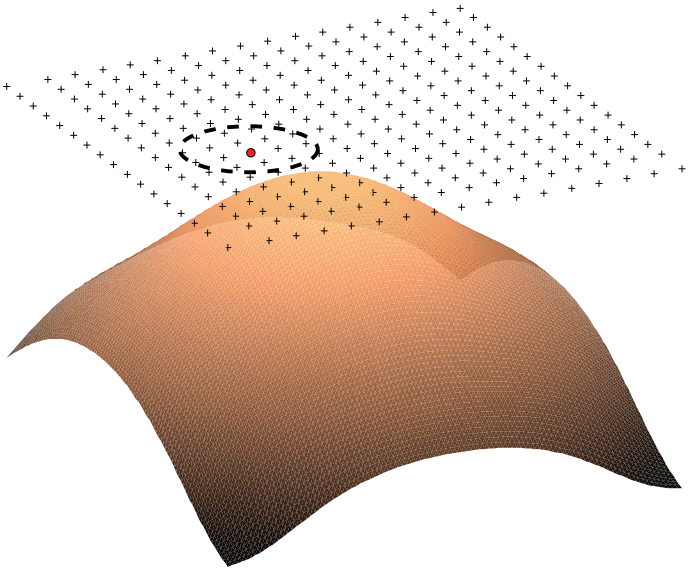

Figure 1: Scheme of the influence domain and the node in which the numerical operations take place.

where θ, α_n, Ψ_n stand for the interpolation function, the number of basis functions, the approximation coefficients and the basis functions, respectively. The basis could be selected arbitrarily, however in this paper only Hardy's multiquadrics (MQs)

$$\Psi_n(\mathbf{p}) = \sqrt{(\mathbf{p}-\mathbf{p}^n)\cdot(\mathbf{p}-\mathbf{p}^n)/\sigma_C^2 + 1}, \tag{6}$$

with σ_C standing for the free shape parameter of the basis function, are used. By taking into account all influence nodes and equation (5), the approximation system is obtained. In this paper the simplest possible case is considered, where the number of influence domain nodes is exactly the same as the number of basis functions. In such a case the approximation simplifies to collocation. The problem is described through a linear system of N equations. The matrix formulation of the collocation is thus

$$\boldsymbol{\Psi\alpha} = \boldsymbol{\Theta}, \tag{7}$$

where

$$\begin{array}{l} \boldsymbol{\Psi} = \begin{bmatrix} \Psi_{11} & \dots & \Psi_{1N_{Sub}} \\ \dots & \dots & \dots \\ \Psi_{N_{Sub}1} & \dots & \Psi_{N_{Sub}N_{Sub}} \end{bmatrix}, \\ \boldsymbol{\alpha} = \begin{bmatrix} \alpha_1 & \dots & \alpha_{N_{Sub}} \end{bmatrix}^{tr}, \\ \boldsymbol{\Theta} = \begin{bmatrix} \Theta_1 & \dots & \Theta_{N_{Sub}} \end{bmatrix}^{tr} \end{array}. \tag{8}$$

The determination of the coefficients is in all discussed cases focused on solving the equation (7)

$$\boldsymbol{\alpha} = \boldsymbol{\Psi}^{-1}\boldsymbol{\Theta}. \tag{9}$$

With the constructed collocation function an arbitrary spatial differential operator (L) can be computed

$$L\theta(\mathbf{p}) = \sum_{n=1}^{N} \alpha_n L\Psi_n(\mathbf{p}). \tag{10}$$

In this work, only five-noded influence domains are used, together with five MQs. The first and the second derivatives are needed when solving the transport type equations, and the respective derivatives of MQ are

$$\frac{\partial}{\partial p_{x,y}}\Psi_n(\mathbf{p}) = \frac{1}{\sigma_C^2}\frac{p_{x,y} - p_{x,y}^n}{\Psi_n^{(}\mathbf{p})}, \tag{11}$$

$$\frac{\partial^2}{\partial p_{x,y}^2}\Psi_n^{MQ}(\mathbf{p}) = \frac{1}{\sigma_C^2}\frac{1}{\Psi_n^{MQ^3}(\mathbf{p})}. \tag{12}$$

In general, the system (7) has to be solved only when the influence domain topology changes and therefore the computation can be optimized by computing $\boldsymbol{\Psi}^{-1}$ in a pre-process. Furthermore, the computation of the coefficients and the evaluation of differential operators can be combined. All information about the numerical approach and the local nodal topology can be stored in a predefined vector, which has to be re-evaluated only when the topology of the nodes changes. The differential operator (χ_m^L) vector is introduced as

$$\chi_m^L(\mathbf{p}) = \sum_{n=1}^{N} \Psi_{nm}^{-1} L\left(\Psi_n(\mathbf{p})\right). \tag{13}$$

The introduced formalism holds in general and therefore the general notation for partial differential operator (L) is used. However, in the present work, only operators $\partial/\partial p_\varepsilon$ and ∇^2 are needed.

$$\chi_m^{\nabla^2}(\mathbf{p}) = \sum_{n=1}^{N} \Psi_{nm}^{-1} \sum_{\varepsilon} \frac{\partial^2}{\partial p_\varepsilon^2} \Psi_n(\mathbf{p}), \tag{14}$$

$$\chi_m^{\partial/\partial p_\varepsilon}(\mathbf{p}) = \sum_{n=1}^{N} \Psi_{nm}^{-1} \frac{\partial}{\partial p_\varepsilon} \Psi_n(\mathbf{p}), \tag{15}$$

$$\chi_m^{1}(\mathbf{p}) = \sum_{n=1}^{N} \Psi_{nm}^{-1} \Psi_n(\mathbf{p}). \tag{16}$$

In equation (16) the interpolation ($L = 1$) operator is introduced as it is needed when new nodes are added to the computational domain.

The structured formulation is convenient since most of the complex and CPU demanding operations are performed in the pre-process phase. For all inner time loop operations only N point operations (FLOPS) are need for evaluation of an arbitrary partial differential operator.

With Euler time stepping and the elaborated spatial discretization scheme the general transport equation (1) can be numerically solved

$$\frac{\Phi_\Omega^1 - \Phi_\Omega^0}{\Delta t} = \nabla D_\Omega^0 \cdot \nabla \Phi_\Omega^0 + D_\Omega^0 \nabla^2 \Phi_\Omega^0 - \nabla \cdot \left(\rho_\Omega^0 \mathbf{v}_\Omega^0\right) \Phi_\Omega^0 - \nabla \Phi_\Omega^0 \cdot \left(\rho_\Omega^0 \mathbf{v}_\Omega^0\right) + S_\Omega^0. \tag{17}$$

where $\Phi_\Omega^{0,1} = \Phi(\mathbf{p}_\Omega, [t_0, t_1])$ and $\mathbf{v}_\Omega^0 = \mathbf{v}^0(\mathbf{p}_\Omega, t_0)$ stand for the field value in the interior node with index Ω at the current and the next time-step.

4 Manipulation of the nodes

The h-adaptivity, developed in the present paper, consists of (I) local refinement/derefinement rules for the nodes, (II) error indicator and (III) triggering of refinement/derefinement with respect to the error indicator and (IV) management of the new local topology. The domain is initially discretized with uniform equidistant node arrangement in all discussed situations (i.e. the basic parent configuration). This assumption, which implies certain restrictions on the shape of the computational domain, is used in the present paper in order to simplify the discussion. This assumption will be relaxed in our future publications. In the case when a certain part of the domain needs higher node density, additional nodes are added, as well

as the unnecessary nodes are removed from the domain, where dense node distribution is not needed. New nodes are added symmetrically around the considered node. A maximum of four additional nodes are positioned in the domain at one refine operation. Examples of refinement and derefinement are presented in Figures 3 and 4. In order to determine in which nodes the refinement should take place an error indicator is introduced. The refinement/derefinement strategy follows the following rules:

Refinement rules:

1. The level of the node marks how many times the node has been refined. The lever zero marks the initial basic parent configuration.

2. The difference between the refinement levels of the neighboring nodes is not allowed to exceed one.

3. In order to support the refinement of the node, the refinement request is passed to all the nodes that block the refinement procedure due to the rule 2.

4. All child nodes are positioned symmetrically around the parent node.

5. If a node A is a neighbor of the node B, than the node B might not be the neighbor of a node A (Figure 2).

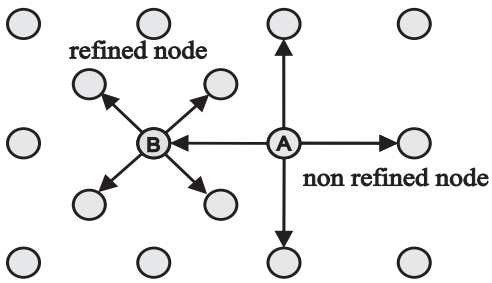

Figure 2: Scheme of the neighbors of the nodes for two nodes with a different refinement level.

Derefinement rules:

1. The initial basic parent configuration nodes (level zero) are not allowed to be removed.

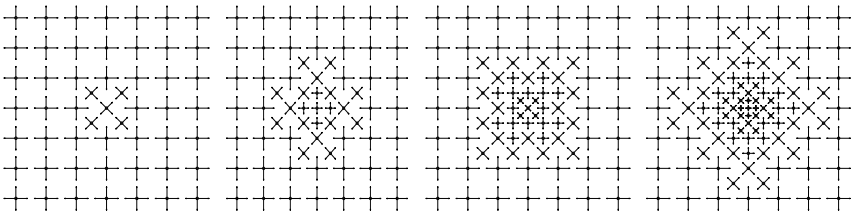

Figure 3: 4 steps sequence of a node refinement.

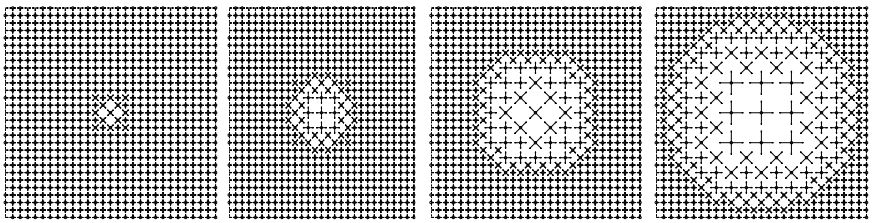

Figure 4: 4 steps sequence of a node derefinement.

2. The level difference between neighbors after a node is derefined is not allowed to exceed one.

3. The node is not allowed to be derefined if after closing an inconsistent distribution regarding the refinement rules would appear.

4. The child node is not allowed to be removed if any other node sees it as a neighbor.

5 Error indication and triggering of node distribution refinement/derefinement

A reliable and efficient error indicator and the associated refinement/derefinement strategy are crucial issues for adaptive calculations. In general, two distinct types of procedures are currently available for deriving error indicators: the recovery based

error indicator and the residual based error indicator. The recovery error indicator was first introduced by Zienkiewicz and Shu in 1987 [Zienkiewicz and Zhu, (1987)] by constructing locally an improved solution from the approximation. The recovery procedure plays an important role in calculation of this indicator. On the other hand, the residual based error indicator [Ainsworth and Oden, (1993)] makes use of the residual of the numerical approximation and offers a very effective alternative.

The basic idea in this paper is to keep all numerical procedures as simple as possible and structured only on the local five-noded topology. Respectively, a suitable, numerically effective local characterization of the node distribution topology and field values is required. The idea of the proposed adaptation criterion is based on the assumption that the numerical error and the instability change with the field complexity and the spatial dimension of the influence domain. Through the numerical experimentation, a straightforward error indication is formulated. The error indicator is in the present collocation method introduced as a norm of the approximation function coefficients, divided by the norm of the approximation function system matrix

$$R_I = \frac{|\boldsymbol{\alpha}|}{|\boldsymbol{\Psi}^{-1}|}, \tag{18}$$

with the norm

$$|\boldsymbol{\Psi}| = \max\left(\sum_{m=1}^{N} |\Psi_{mi}|\right); i = 1,2,...,N, \tag{19}$$

defined as the largest absolute column sum. The refinement/derefinement criteria is thus formulated as

$$\begin{aligned} &\text{if } R_l > \sigma_R^{hi} \rightarrow && \text{refine node} \\ \text{if } \sigma_R^{hi} \geq R_l \geq \sigma_R^{lo} &\rightarrow && \text{preserve node} \\ &\text{if } R_l < \sigma_R^{lo} \rightarrow && \text{derefine node} \end{aligned} \tag{20}$$

The nodes where the refinement indicator is within the allowed interval $\left(R_I^{\min}, R_I^{\max}\right)$ stay intact, otherwise the action is taken into account with respect to the presented logic (20). Furthermore, the refinement algorithm is limited by the maximum number of refinement level $(\sigma_R^{\max})$ allowed for the highest node distribution density, and with the initial node distribution for the lowest node distribution density.

After the refinement action, new node field values are set through the approximation from the local influence domain.

$$\Theta(\mathbf{p}) = \sum_{m=1}^{N_{Sub}} \chi_m^1(\mathbf{p})\, \Theta_m. \tag{21}$$

In order to illustrate the refinement procedure, a known test field with a step jump, mimicking the problematic field distribution (Figure 7), is subjected to the refinement procedure (Figure 8). The contour plots in figures represent the refinement indicator. Within the area of higher gradients in the field, the refinement indicator is high and therefore more nodes are added in order to lower it, while within the plain areas of the domain, the refinement indicator is low and therefore nodes relax to the minimal possible node distribution density, i.e. initial distribution. After the refinement, the indicator is below the prescribed value within the whole domain and the areas with the high indicator before refinement are covered with much denser node distribution. In the present illustrative case the $\sigma_R^{hi} = 1.00$ (top left plot), $\sigma_R^{hi} = 0.15$(top right plot), $\sigma_R^{hi} = 0.10$(bottom left plot) and $\sigma_R^{hi} = 0.05$ (bottom right plot) with 265, 503, 811 and 2212 nodes, respectively, are shown. The maximum allowed refinement $\sigma_R^{\max} = 10$ is used for all four plots with the test field defined as (note that the tilde is used to denote a dimensionless value, the same notation will be used in further discussions, as well).

$$f = \frac{1 - \tanh(10\sin(1.8\tilde{p}_x) - 10\,\tilde{p}_y - 2.6)}{2}. \tag{22}$$

6 Numerical example

In the present paper the time dependent Burgers' equation is considered as a special case of the general transport equation. The equation with convection, viscous and time dependent terms is similar to the Navier-Stokes equation without pressure gradient term. The Burgers' equation was originally employed in weather problems and later extended to more complex models of turbulent flows [Burgers, (1948)]. The Burgers' equation is used to model several physical phenomena like shock waves, acoustics, various flow problems, etc. The equation behaves parabolic when viscosity term is dominant and hyperbolic otherwise. The sharp discontinuities might appear in the solution of the problem due to the nonlinearity of the Burgers' equation and this behavior makes the equation suitable for testing of the numerical methods. Moreover, this behavior makes the test ideal for assessment of node refinement strategy due to sharp jump in the solution.

There exists quite a large amount of publications [Bahadir, (2003); Özis, Esen and Kutluay, (2005); Perko, (2007); Saka and Dag, (2008); Young, Fan, Hu and Atluri, (2008); Zhang, Ouyang and Zhang, (2009); Abazari and Borhanifar, (2010)] on the solution of the Burgers' equation. The Burgers equation was previously solved by the following related meshless techniques [Shi, Shu, Song and Zhang, (2005); Hashemiana and Shodja, (2008); Hosseini, Hashemi and (2011)]. This makes the test even more attracting; as it provides additional evaluation of the present numerical approach through comparison with the others.

A two dimensional Burgers' equation on a square domain of the dimensionless size 1x1 (Figure 7) is considered

$$\frac{\partial \mathbf{v}}{\partial t} + \mathbf{v} \cdot \nabla \mathbf{v} = \frac{1}{Re} \nabla^2 \mathbf{v}, \tag{23}$$

where Re stands for Reynolds number. The problem can be solved in a closed form [Fletcher, (1983)]

$$\mathbf{v}^a(\mathbf{p},t) = \begin{pmatrix} \frac{3}{4} - \frac{1}{4}\left(1 + e^{-1\frac{4p_x - 4p_y + t}{32}Re}\right)^{-1} \\ \frac{3}{4} + \frac{1}{4}\left(1 + e^{-1\frac{4p_x - 4p_y + t}{32}Re}\right)^{-1} \end{pmatrix}, \tag{24}$$

where $\mathbf{v}^a$ stands for the analytical solution. The initial state and Dirichlet boundary conditions are derived from the solution $\mathbf{v}^a$ (24).

Numerical implementation of the developed solution procedure is coded in C++ programming language in double precision and compiled with Intel C++ v. 11.1 compiler. The LAPACK (Linear algebra package) routines are used to solve the LU decomposition. The standard C++ libraries are used for other mathematical and system operations needed to complete the solver. Recently it was demonstrated that the proposed local meshless based solution procedure can be effectively parallelized with OpenMP [Kosec, Trobec, Depolli and Rashkovska, (2011)].

7 Results

We solve the Burger's equation with the described adaptive solution procedure. The maximum absolute error is defined as

$$\mathrm{E} = \max\left(|v_x^a(\mathbf{p}_\Omega,t) - v_x(\mathbf{p}_\Omega,t)|\right). \tag{25}$$

For computation of errors, all domain nodes are taken into account. First, four different uniform node distributions are tested for Reynolds numbers 10^2 and 10^3 with respect to time (Figure 8).

The results with 957, 2597, 10197 and 40397 regular node distributions are computed with time-steps 10^{-4}, $5 \cdot 10^{-5}$, 10^{-5}, and 10^{-6}, respectively.

Furthermore, the results, computed with the proposed meshless method, are compared with a selection of reasonably well documented published data. The results of global radial basis collocation method [Ali, ul-Islam and Haq, (2009)] - Ref 1, implicit finite difference method [Bahadir, (2003)] - Ref 2 and the Eulerian-Lagrangian method of fundamental solution [Young, Fan, Hu and Atluri, (2008)] - Ref 3 are compared against present results in Table 1. The comparison case is

Re=100 on a 437 uniformly distributed nodes where for the present results a time-step 10^{-4} is used. From the comparison it is evident that the proposed approach shows good agreement with respect to the reference numerical data.

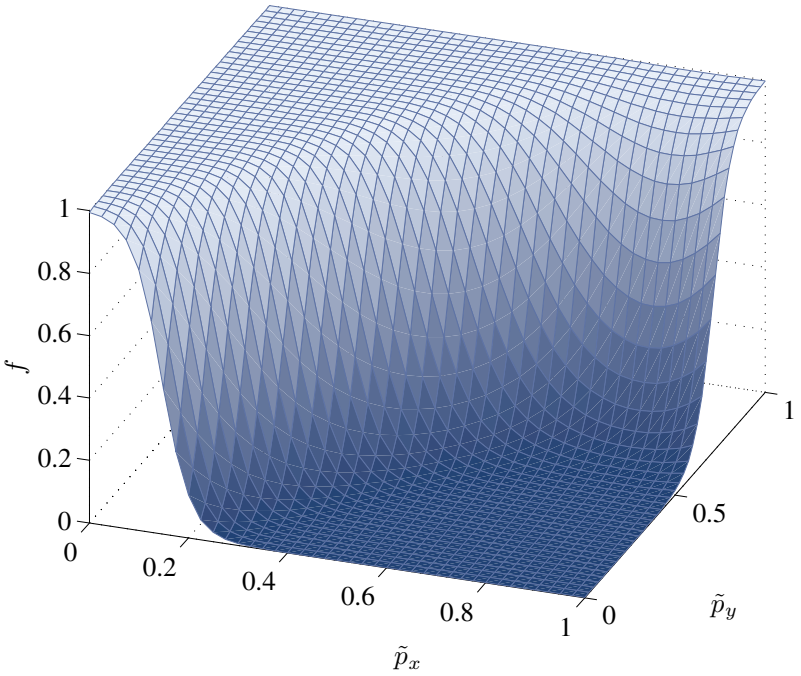

Figure 3: Test function for demonstration of refinement.

The second part of the analysis is focused on the application of the adaptive node distribution strategy. The behavior of case $Re = 10^3$ with respect to different adaptivity settings is considered. An example of transient node distribution propagation is shown in Figure 9. Three different settings of node distribution adaptivity are compared with the static node distribution computation. All cases are computed with the same average number of the nodes (2601) through all the simulation in order to keep the comparison reasonable. The numerical setup information is listed in Table 2. All adaptive computations are done with time-step 10^{-5}. To illustrate the impact of adaptivity setup on the actual node distribution, the distributions after the first refinement for all three adaptive cases are plotted in Figure 10. The comparison of static against adaptive node distribution computation is presented in Figure 11.

Table 1: A comparison of present adaptive method data with published data.

	$\tilde{v}_x$					$\tilde{v}_y$				
$\tilde{\mathbf{p}}$	exact	present	ref 1	ref 2	ref 3	exact	present	ref 1	ref 2	ref 3
(0.1,0.1)	0.50048	0.50047	0.50035	0.49983	0.50012	0.99951	0.99953	0.99936	0.99826	0.99946
(0.5,0.1)	0.50000	0.50000	0.50002	0.49930	0.49996	0.99999	0.99999	1.00011	0.99860	0.99980
(0.3,0.3)	0.50048	0.50044	0.50042	0.49977	0.50042	0.99951	0.99955	0.99951	0.99861	0.99938
(0.7,0.3)	0.50000	0.50000	0.50003	0.49930	0.49999	0.99999	0.99999	1.00011	0.99860	0.99984
(0.5,0.5)	0.50048	0.50041	0.50046	0.49973	0.50041	0.99951	0.99958	0.99958	0.99821	0.99941
(0.9,0.5)	0.50000	0.50000	0.50002	0.49931	0.49999	0.99999	0.99999	1.00009	0.99862	0.99984
(0.3,0.7)	0.55567	0.55480	0.55609	0.55429	0.55587	0.94432	0.94519	0.94387	0.94409	0.94387
(0.7,0.7)	0.50048	0.50038	0.50048	0.49970	0.50045	0.99951	0.99961	0.99961	0.99823	0.99937
(0.1,0.9)	0.74425	0.74419	0.74409	0.74340	0.74416	0.75574	0.75580	0.75592	0.75500	0.75558
(0.5,0.9)	0.55567	0.55448	0.55604	0.55413	0.55637	0.94432	0.94551	0.94392	0.94441	0.94345

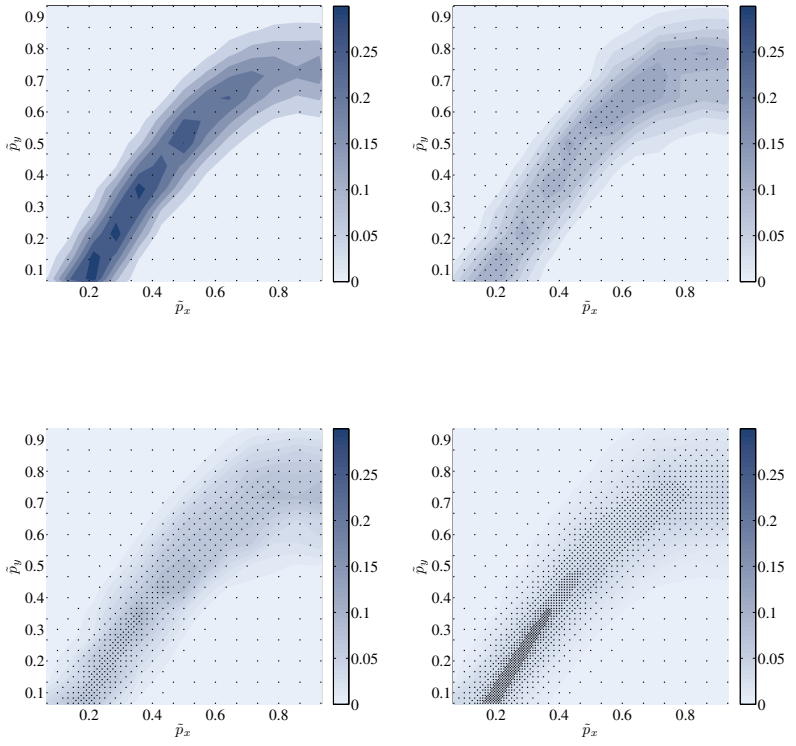

Figure 4: An example of different refinement settings with the contour plot standing for the refinement indicator. From no refinement situation on the top left figure to more refined distribution on the bottom right figure.

As expected, the discretizations with nodes refined near the jump, perform better. From $adap1$ to $adap3$ the discretizations with lower to higher density near the jump are tested. The higher is the concentration of the nodes near the jump, the better performance is achieved. The behavior is expected, since the maximum error is always within the area of the jump, while the other parts of the domain are not subjected to intense computations, and are producing much lower errors.

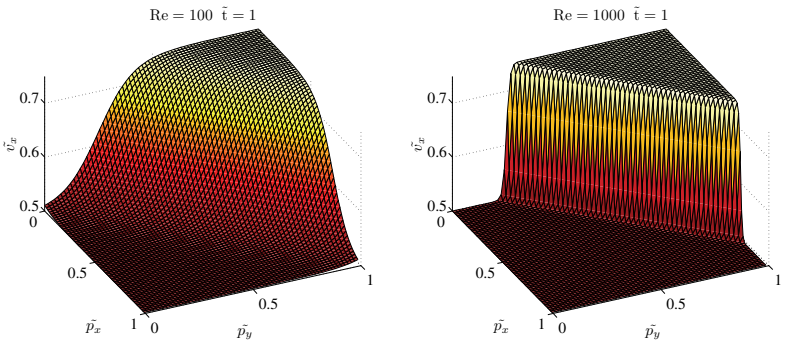

Figure 5: Solution of Burgers' equation for Re=100 (left) and Re=1000 (right).

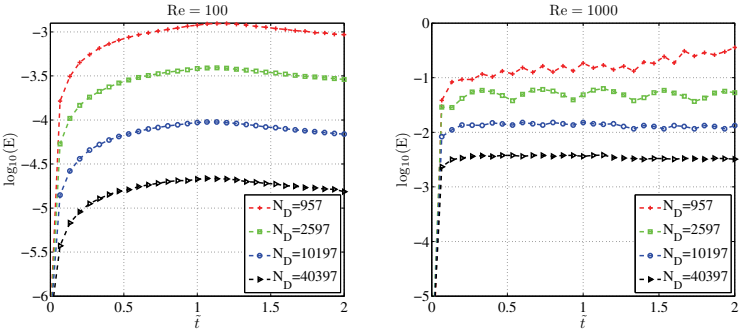

Figure 6: Error as a function of time for Re=100 (left) and Re=1000 cases.

Table 2: The configuration parameters of the numerical method when solving Burgers' equation

	*stat*1	*adap*1	*adap*2	*adap*3
$\sigma_R^{\max}$	0	2	4	6
N_D	2597	1596	780	320
σ_R^{lo}	0	0.0005	0.0010	0.0050
σ_R^{hi}	0	0.0010	0.0050	0.0150
$\sigma_R^{N_t}$	0	100	100	100

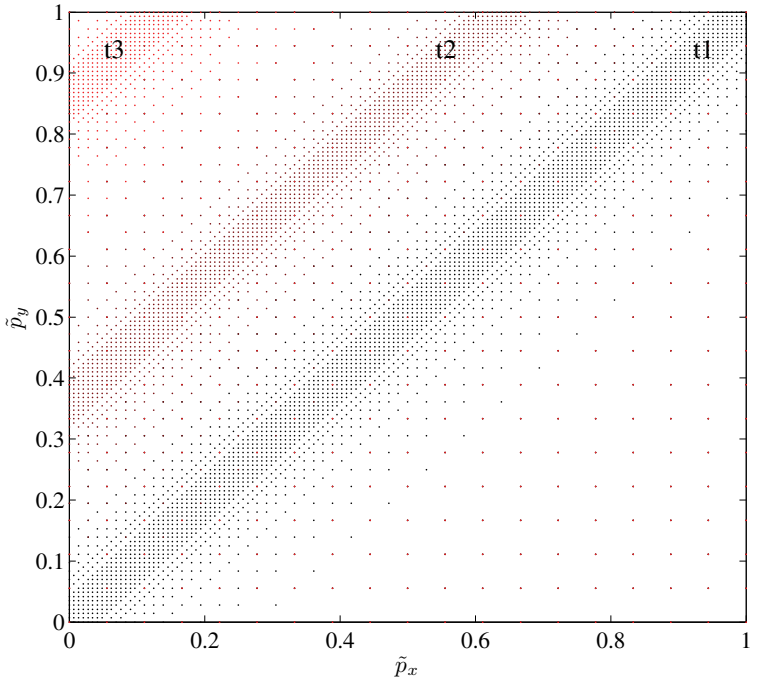

Figure 7: Node distributions at three different times $\tilde{t} = [0, 1.5, 3.5]$ for adaptive numerical example *adap*3.

8 Conclusions

The local meshless radial basis function collocation method, combined with the local adaptive node distribution strategy, has been formulated for transport type equations in the present paper. There are at least two important distinct elements of the developments shown, differing from other strong form adaptive meshless method attempts: (I) A five noded collocation is preserved in all situations. This feature is enabled by a smart nesting of the added and removed nodes. (II) The error indicator is defined in an unique and simple way through the collocation coefficients vector and collocation matrix norm. The LRBFCM solution procedure has been rewritten and afterwards coded in terms of partial differential vectors in order to optimize the computations as much as possible. The assessment of the method is done through the well-known Burgers' equation, where the performance is quantitatively compared against other numerical approaches found in the literature. The Burgers'

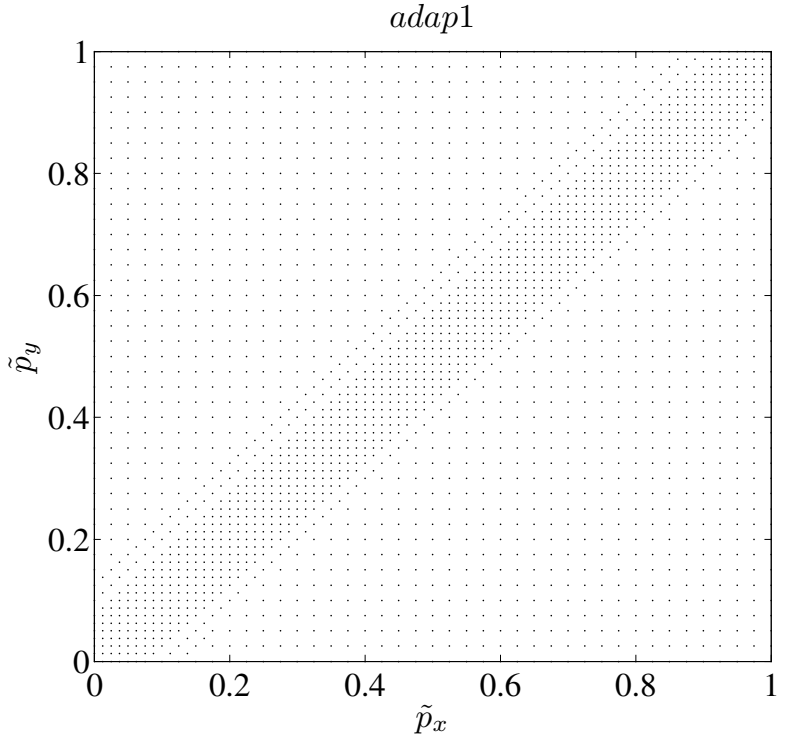
$adap1$
1
0.8
0.6
0.4
0.2
0
$\tilde{p}_y$
0
0.2
0.4
0.6
0.8
1
$\tilde{p}_x$

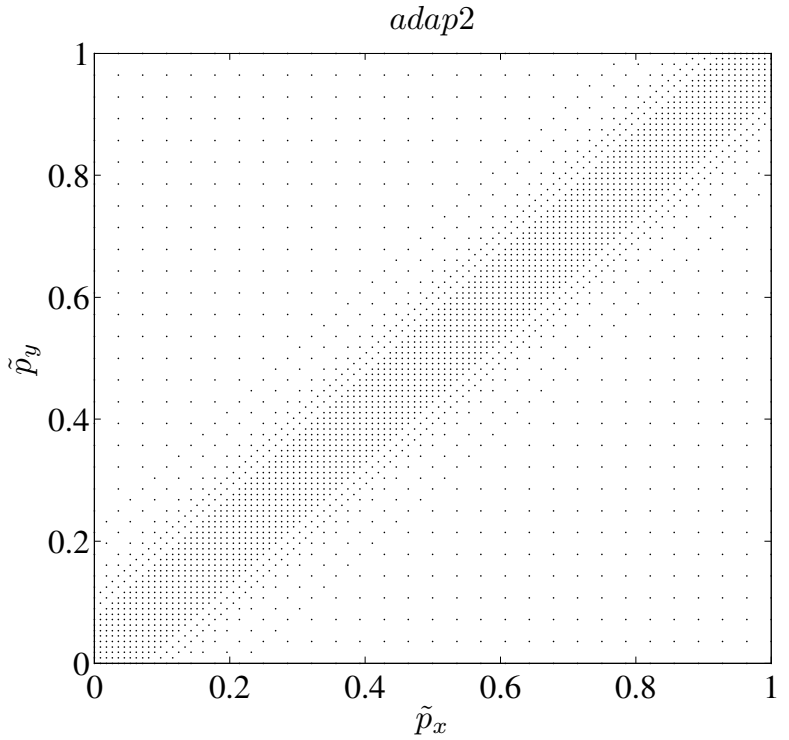
$adap2$
1
0.8
0.6
0.4
0.2
0
$\tilde{p}_y$
0
0.2
0.4
0.6
0.8
1
$\tilde{p}_x$

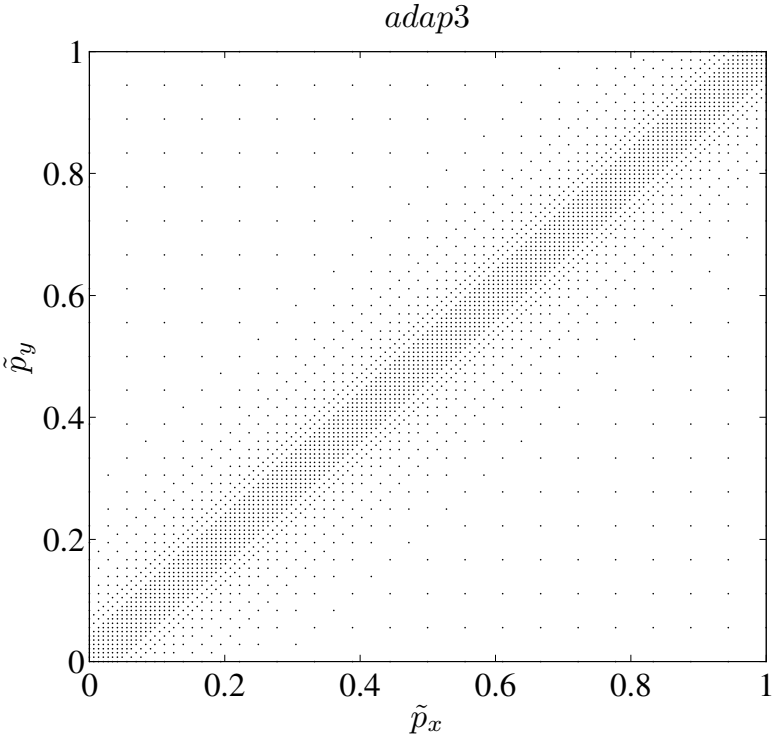

Figure 8: Node distributions for *adap*1-3 cases after the first time step.

equation example is used to assess the adaptive node distribution approach. As it is shown in the presented analysis, the procedure behaves as expected and significantly improves the performance of the basic numerical method without adaptive features. Our forthcoming publication will deal with the extension of the method to arbitrary shaped 2D domains and moving boundary problems, associated with solidification, as appear in many materials processing situations.

Acknowledgement: The authors would like to express their gratitude to Slovenian Research Agency for support in the framework of the projects Young Researcher Programme 1000-06-310232, project J2-4120 Advanced modeling of solid-liquid systems, and programme group P2-0379 Modeling and Simulation of Materials and Processes. The Centre of Excellence for Biosensors, Instrumentation and Process Control is an operation financed by the European Union, European Regional Development Fund and Republic of Slovenia, Ministry of Higher Educa-

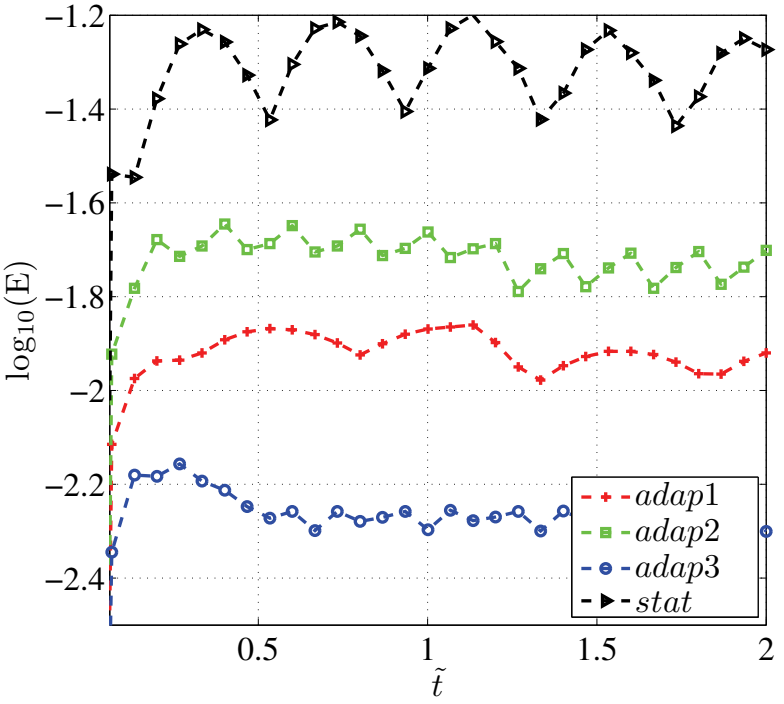

Figure 9: Comparison of static and three adaptive node distribution computations.

tion, Science and Technology.

References

Abazari, R.; Borhanifar, A. (2010): Numerical study of the solution of the Burgers and coupled Burgers equations by a differential transformation method. *Computers & Mathematics with Applications*, vol. 59, pp. 2711-2722.

Ainsworth, M.; Oden, J.T. (1993): A unified approach to a posteriori error estimation using element residual methods. *Numerische Mathematik*, vol. 65, pp. 23-50.

Ali, A.; ul-Islam, S.; Haq, S. (2009): A computational meshfree technique for the numrecial solution of two-dimensional coupled Burger's equation. *International Journal for Computational Methods in Engineering Science and Mechanics*, vol. 10, pp. 406-422.

Atluri, S. N. (2004): *The Meshless Method (MLPG) for Domain and BIE Discretization,* Tech Science Press, Forsyth.

Atluri, S. N.; Shen, S. (2002): The meshless local Petrov-Galerkin (MLPG) method: a simple & less-costly alternative to the finite element and boundary element methods. *CMES: Computer Modeling in Engineering & Sciences*, vol. 3, pp. 11-52.

Bahadir, A. R. (2003): A fully implicit finite-difference scheme for two-dimensional Burgers' equations. *Applied Mathematics and Computation*, vol. 137, pp. 131-137.

Behrens, J; Iske, A. (2002): Grid-free adaptive semi-Lagrangian advection using radial basis functions. *Computers & Mathematics with Applications*, vol. 43, pp. 319-327.

Berger, M. J. (1983): Adaptive mesh refinement for hyperbolic partial differential equations. *Journal of Computational Physics*, vol. 53, pp. 484-512.

Berger, M. J.; Colella, P. (1989): Local adaptive mesh refinement for shock hydrodynamics. *Journal of Computational Physics*, vol. 82, pp. 64-84.

Bourantas, G. C.; Skouras, E. D.; Nikiforidis, G. C. (2009): Adaptive support domain implementation on the moving least squares approximation for MFree methods applied on elliptic and parabolic PDE problems using strong-form description. *CMES: Computer Modeling in Engineering & Sciences*, vol. 43, pp. 1-25.

Buhmann, M. D. (2000): *Radial Basis Functions,* Cambridge University Press, Cambridge.

Burgers, J. M. (1948): A Mathematical Model Illustrating the Theory of Turbulence*, Advances in Applied Mechanics,* Elsevier, pp. 171-199.

Chen, C. S.; Ganesh, M.; Golberg, M. A.; Cheng, A. H. D. (2002): Multilevel compact radial basis functions based computational scheme for some elliptic problems. *Computers and Mathemathics with Applications*, vol. 43, pp. 359-378.

Divo, E.; Kassab, A. J. (2007): Localized meshless modeling of natural-convective viscous flows. *Numerical Heat Transfer*, vol. B129, pp. 486-509.

Fasshauer, G. (2006): Radial basis functions and related multivariate meshfree approximation methods: Theory and applications - Preface. *Computers & Mathematics with Applications*, vol. 51, pp. 1223-1366.

Fletcher, J. D. (1983): Generating exact solutions of the two-dimensional Burgers' Equations. *International Journal for Numerical Methods in Fluids*, vol. 3, pp. 213-216.

Gan, NF; Li, GY; Long, SY (2009): 3D adaptive RKPM method for contact problems with elastic–plastic dynamic large deformation. *Engineering Analysis with Boundary Elements*, vol. 33, pp. 1211-1222.

Haq, S.; ul-Islam, S.; Arshed, A. (2008): A numerical meshfree technique for the solution of the MEW equation. *CMES: Computer Modeling in Engineering & Sciences*, vol. 38, pp. 575-599.

Hashemiana, A.; Shodja, HM. (2008): A meshless approach for solution of Burgers' equation. *Journal of Computational and Applied Mathematics* vol. 220, pp. 226-239.

Hosseini, B.; Hashemi, R.; (2011): *International Journal for Computational Methods in Engineering Science and Mechanics*, vol. 12, pp. 44-58.

Kansa, E. J. (1990a): Multiquadrics - a scattered data approximation scheme with application to computational fluid dynamics, part I. *Computers and Mathematics with Applications*, vol. 19, pp. 127-145.

Kansa, E. J. (1990b): Multiquadrics - a scattered data approximation scheme with application to computational fluid dynamics, part II. *Computers and Mathematics with Applications*, vol. 19, pp. 147-161.

Kee, B.B.T. ; Liu, G.R.; Lu, C. (2008): A least-square radial point collocation method for adaptive analysis in linear elasticity. *Engineering Analysis with Boundary Elements*, vol. 32, pp. 440-460.

Kosec, G.; Šarler, B. (2008a): Solution of thermo-fluid problems by collocation with local pressure correction. *International Journal of Numerical Methods for Heat and Fluid Flow*, vol. 18, pp. 868-882.

Kosec, G.; Šarler, B. (2008b): Local RBF collocation method for Darcy flow. *CMES: Computer Modeling in Engineering & Sciences*, vol. 25, pp. 197-208.

Kosec, G.; Šarler, B. (2009): Solution of phase change problems by collocation with local pressure correction. *CMES: Computer Modeling in Engineering & Sciences*, vol. 47, pp. 191-216.

Kosec, G.; Trobec, R.; Depolli, M.; Rashkovska, A. (2011): Multicore parallelization of a meshless PDE solver with OpenMP, *ParNum 11, Leibnitz.*

Kovačevič, I.; Poredoš, A.; Šarler, B. (2003): Solving the Stefan problem with the radial basis function collocation method. *Numerical Heat Transfer*, vol. B44, pp. 575-599.

Kovačevič, I.; Šarler, B. (2005): Solution of a phase-field model for dissolution of primary particles in binary aluminum alloys by an r-adaptive mesh-free method. *Materials Science and Engineering* vol. A413-414, pp. 423-428.

Le, P.; Mai-Duy, N; Tran-Cong, T.; Baker, G. (2008): A meshless modeling of dynamic strain localization in quasi-brittle materials using radial basic function networks. *CMES: Computer Modeling in Engineering & Sciences*, vol. 25, pp. 43-66.

Lee, C. K. ; Liu, X.; Fan, S.C. (2003): Local muliquadric approximation for solving boundary value problems. *Computational Mechanics*, vol. 30, pp. 395-409.

Li, S.; Petzold, L.; Ren, Y. (1998): Stability of moving mesh systems of partial differential equations. *Journal of Scientific Computing*, vol. 20, pp. 719-738.

Libre, A. L.; Emdadi, A.; Kansa, E. J.; Shekarchi, M.; Rahimian, M. (2008): A fast adaptive wavelet scheme in RBF collocation for nearly singular potential PDEs. *CMES: Computer Modeling in Engineering & Sciences*, vol. 38, pp. 263-284.

Libre, N. A.; Emdadi, A.; Kansa, E. J.; Rahimian, M.; Shekarchi, M. (2008): A stabilised RBF collocation scheme for Neumann type boundary conditions. *CMES: Computer Modeling in Engineering & Sciences*, vol. 24, pp. 61-80.

Ling, L.: (2011): An adaptive-hybrid meshfree approximation method. *International Journal for Numerical Methods in Engineering*, 10.1002/nme.3257.

Liu, G; Huynh, D; Gu, Y. (2006): An adaptive meshfree collocation method for static and dynamic nonlinear problems*, Computational Methods,* Springer, pp. 1459–1464.

Liu, G. R.; Gu, Y. T. (2001): A point interpolation method for two-dimensional solids. *International Journal for Numerical Methods in Engineering*, vol. 50, pp. 937-951.

Liu, G.R. ; Wu, Y.L.; Ding, H. (2004): Meshfree weak-strong (MWS) form method and its application to incompressible flow problems. *International Journal of Numerical Methods in Fluids*, vol. 46, pp. 1025-1047.

Liu, G.R.; Kee, B.B.T.; Lu, C. (2006): A stabilized least-squares radial point interpolation method (LS-RPCM) for adaptive analysis. *Computer Methods in Applied Mechanics and Engineering*, vol. 195, pp. 4843-4861.

Lorbiecka, A. Z.; Šarler, B. (2010): Simulation of dendritic growth with different orientation by using the point automata method. *CMC: Computers, Materials & Continua*, vol. 18, pp. 69-103.

Mai-Cao, L.; Tran-Cong, T. (2005): A meshless IRBFN-based method for transient problems. *CMES: Computer Modeling in Engineering & Sciences*, vol. 7, pp. 149-171.

Mai-Cao, L.; Tran-Cong, T. (2008): A meshless approach to capturing moving interfaces in passive transport problems. *CMES: Computer Modeling in Engineering & Sciences*, vol. 31, pp. 157-188.

Mai-Duy, N. ; Tran-Cong, T. (2002): Mesh-free radial basis function network methods with domain decomposition for approximation of functions and numerical

solution of Poisson's equations. *Engineering Analysis with Boundary Elements*, vol. 26, pp. 133-156.

Mai-Duy, N.; Khennane, A.; Tran-Cong, T. (2007): Computation of laminated composite plates using integrated radial basis function networks *CMC: Computers, Materials & Continua*, vol. 5, pp. 63-78.

Mai-Duy, N.; Mai-Cao, L.; Tran-Cong, T. (2007): Computation of transient viscous flows using indirect radial basic function networks. *CMES: Computer Modeling in Engineering & Sciences*, vol. 18, pp. 59-77.

Mai-Duy, N.; Tran-Cong, T. (2003): Indirect RBFN method with thin plate splines for numerical solution of differential equations. *CMES: Computer Modeling in Engineering & Sciences*, vol. 4, pp. 85-102.

Mencinger, J. (2003): Numerical simulation of melting in two-dimensional cavity using adaptive grid. *Journal of Computational Physics*, vol. 198, pp. 243-264.

Monaghan, J. J. (1988): An Introduction to SPH. *Computer Physics Communications*, vol. 48, pp. 89-96.

Özis, T.; Esen, A.; Kutluay, S. (2005): Numerical solution of Burgers' equation by quadratic B-spline finite elements. *Applied Mathematics and Computation*, vol. 165, pp. 237-249.

Park, S. H.; C., Kwon K.; K., Youn S. (2003): A posteriorierror estimates and an adaptive scheme of least-squares meshfree method. *Internation Journal of Numerical Methods in Engineering*, vol. 58, pp. 1213-1250.

Perko, J.; Šarler, B. (2007): Weight function shape parameter optimization in meshless methods for non-uniform grids. *CMES: Computer Modeling in Engineering & Sciences*, vol. 19, pp. 55-68.

Prax, C.; Sadat, H.; Salagnac, P. (1996): Diffuse approximation method for solving natural convection in porous Media. *Transport in Porous Media*, vol. 22, pp. 215-223.

Rabczuk, T.; Belytschko, T. (2005): Adaptivity for structured meshfree particle methods in 2D and 3D. *Internation Journal of Numerical Methods in Engineering*, vol. 63, pp. 1559-1582.

Saka, B.; Dag, I. (2008): A numerical study of the Burgers' equation. *Journal of the Franklin Institute*, vol. 345, pp. 328-348.

Sanyasiraju, Y.V.S.S.; Chandhini, G. (2008): Local radial basis function based gridfree scheme for unsteady incompressible viscous ?ows. *Journal of Computational Physics*, vol. 227, pp. 9822-8924.

Shanazari, K. ; Rabie, N. (2009): A three dimensional adaptive nodes technique applied to meshless-type methods. *Applied Numerical Mathematics*, vol. 59, pp.

Shi, BJ; Shu, DW; Song, SJ; Zhang, YM (2005): Solving Burgers' equation by a meshless method. *Modern Physics Letters B*, vol. 19, pp. 1651–1654.

Sorić, J.; Jarak, T. (2010): Mixed meshless formulation for analysis of shell-like structures. *Comupter Methods in Applied Mechanics and Engineering*, vol. 199, pp. 1153-1164.

Stevens, D.; Power, H.; Lees, M.; Morvan, H. (2009): The use of PDE data-centres on the local hermitian interpolation meshless method for the numerical solution of convective-diffusion problems. *Journal of Computational Physics*, vol. 228, pp. 4606-4624.

Šarler, B. (2005): A radial basis function collocation approach in computational fluid dynamics. *CMES: Computer Modeling in Engineering & Sciences*, vol. 7, pp. 185-193.

Šarler, B. (2007): From global to local radial basis function collocation method for transport phenomena*, Advances in Meshfree Techniques,* Springer, Berlin, pp. 257-282.

Šarler, B.; Kosec, G.; Lorbiecka, A. Z.; Vertnik, R. (2009): A meshless approach in solution of multiscale solidification modeling. *Materials Science Forum*, vol. 649, pp. 211-216.

Šarler, B.; Perko, J.; Chen, C. S. (2004): Radial basis function collocation method solution of natural convection in porous Media. *International Journal of Numerical Methods for Heat & Fluid Flow*, vol. 14, pp. 187-212.

Šarler, B.; Perko, J.; Chen, C. S.; Kuhn, G. (2001): A meshless approach to natural convection, *International Conference on Computational Engineering and Sciences, CD proceedings.*

Šarler, B.; Vertnik, R. (2006): Meshfree explicit local radial basis function collocation method for diffusion problems. *Computers and Mathematics with Applications*, vol. 51, pp. 1269-1282.

Trobec, R.; Kosec, G.; Šterk, M.; Šarler, B. (2012): Comparison of local weak and strong form meshless methods for 2-D diffusion equation. *Engineering Analysis with Boundary Elements*, vol. 36, pp. 310-321.

Trobec, R.; Sterk, M.; Robic, B. (2009): Computational complexity and parallelization of the meshless local Petrov-Galerkin method. *Computers & Structures*, vol. 87, pp. 81-90.

Vertnik, R; Šarler , B. (2011): Local collocation approach for solving turbulent combined forced and natural convection problems. *Adv. appl. math. mech*, vol. 3, pp. 259-279.

Vertnik, R.; Šarler, B. (2006): Meshless local radial basis function collocation

method for convective-diffusive solid-liquid phase change problems. *International Journal of Numerical Methods for Heat and Fluid Flow*, vol. 16, pp. 617-640.

Vertnik, R.; Šarler, B. (2009): Solution of incompressible turbulent flow by a mesh-free method. *CMES: Computer Modeling in Engineering & Sciences*, vol. 44, pp. 65-95.

Vertnik, R.; Založnik, M.; Šarler, B. (2006): Solution of transient direct-chill aluminium billet casting problem with simultaneous material and interphase moving boundaries by a meshless method. *Engineering Analysis with Boundary Elements*, vol. 30, pp. 847-855.

Wang, J. G.; Liu, G. R. (2002): A point interpolation meshless method based on radial basis functions. *International Journal for Numerical Methods in Engineering*, vol. 54, pp. 1623-1648.

Young, D. L.; Fan, C. M.; Hu, S. P.; Atluri, S. N. (2008): The Eulerian-Lagrangian method of fundamental solutions for two-dimensional unsteady Burgers' equations. *Engineering Analysis with Boundary Elements*, vol. 32, pp. 395-412.

Zerroukat, M.; Power, H.; Chen, C. S. (1998): A numerical method for heat transfer problems using collocation and radial basis functions. *International Journal of Numerical Methods in Engineering*, vol. 42, pp. 1263-1278.

Zhang, X. H.; Ouyang, J.; Zhang, L. (2009): Element-free characteristic Galerkin method for Burgers' equation. *Engineering Analysis with Boundary Elements*, vol. 33, pp. 356-362.

Zienkiewicz, O.C.; Zhu, J.C. (1987): A simple error estimator and adaptive procedure for practical engineering analysis. *International Journal of Numerical Methods in Engineering*, vol. 142, pp. 337-357.